

Article

A Simulation-Based Experimental Design for Analyzing Energy Consumption and Order Tardiness in Warehousing Systems

Hyun-woo Jeon ^{1,*} , Ahmad Ebrahimi ² and Ga-hyun Lee ¹ 

¹ Department of Industrial & Management Systems Engineering, Kyung Hee University, Yongin-si 17104, Republic of Korea

² Department of Mechanical and Industrial Engineering, Louisiana State University, Baton Rouge, LA 70803, USA

* Correspondence: hwjeon@khu.ac.kr; Tel.: +82-31-201-3662

Abstract: For warehouses to be more sustainable and cost-effective, it is essential to consider energy consumption (EC) and order tardiness (OT) together in evaluating warehouse activities since improving both EC and OT at the same time is very demanding. While existing studies try to improve EC and OT, the current studies consider only either a reserve area or a forward area between the two major warehouse areas. Thus, this study proposes a simulation-based approach to assessing EC and OT when reserve and forward areas are considered together in one framework for different configurations of five important warehousing parameters: (i) number of forklifts, (ii) number of storage/retrieval (S/R) machines, (iii) number of automated storage/retrieval systems (AS/RS) input/output (I/O) points, (iv) order size, and (v) proportions of order flows through a reserve or forward area. In particular, we use real forklift movement and energy data for our simulation models to provide a more realistic analysis. By building the simulation model with the 2⁵ full factorial experimental design, we analyze the results with analysis of variance (ANOVA). The resulting Pareto-optimal solutions show that less traffic flows through a reserve area can help improve both EC and OT while other factors have smaller or limited effects on the two responses. Also, the order flow factor has the largest effect on EC while order size has the largest effect on OT. The results from this study can help warehouse operators make informed decisions in considering and finding a trade-off between sustainability and customer satisfaction.

Keywords: energy consumption; order tardiness; simulation-based experiments



check for updates

Citation: Jeon, H.-w.; Ebrahimi, A.; Lee, G.-h. A Simulation-Based Experimental Design for Analyzing Energy Consumption and Order Tardiness in Warehousing Systems. *Sustainability* **2023**, *15*, 14891. <https://doi.org/10.3390/su152014891>

Academic Editor: Armando Carteni

Received: 17 September 2023

Revised: 9 October 2023

Accepted: 12 October 2023

Published: 15 October 2023



Copyright: © 2023 by the authors. Licensee MDPI, Basel, Switzerland. This article is an open access article distributed under the terms and conditions of the Creative Commons Attribution (CC BY) license (<https://creativecommons.org/licenses/by/4.0/>).

1. Introduction

Due to the recent expansion of e-commerce, fast warehousing and fulfillment are catching more attention than before, and both customers and warehouse operators want to avoid order tardiness (OT) and uncertainty as much as possible [1,2]. At the same time, energy consumption (EC) becomes an important aspect of warehousing to consider as sustainable aspects of warehousing are highlighted [2–4]. While EC and OT are worth improving in warehouses, it is a challenging task to improve these targets simultaneously; a reduction in EC can deteriorate OT whereas a decrease in OT is likely to increase EC and relevant costs. Thus, EC and OT in warehouses need to be studied and improved in one integrated framework.

Generally, a warehouse consists of two main functional areas: (i) a reserve area and (ii) a forward area [5,6]. This fact suggests that these two major warehouse areas need to be considered to make the best operational decisions for improving EC and OT. Most current relevant studies, however, focus just on either a reserve area or a forward area, implying that existing relevant studies are somehow insufficiently developed. Accordingly, interactions among these two areas have not been thoroughly studied for EC and OT. Thus, to identify significant warehouse operational factors and examine their individual or

combined effects on EC and OT, a new study needs to be performed by integrating reserve and forward areas so that we can consider most warehouse activities. For these purposes, a simulation study is useful since we can test various configurations of warehouse factors and parameters by checking the effects of the factors on OT and EC as well as the trade-off of the two targets [7,8].

2. Literature Review

Warehousing is the process of temporarily storing stock-keeping units (SKUs) between suppliers (manufacturers), and consumers; its main activities include retrieving, put-away, replenishment, order picking, sortation, cross-docking, and shipping [6]. Receiving is to unload SKUs at inbound decks, inspect the SKUs, and update the inventory records. Put-away is to transfer the SKUs between different areas. Replenishment is to move the SKUs from a reserve area to a forward area. Order picking is to retrieve distinct SKUs from storage locations. Sortation is to group customer orders that have been picked in different batches. Packing is to put the sorted customer orders into a container. Cross-docking is to transfer SKUs directly from inbound to outbound decks. Shipping is to inspect the packed customer orders, update the inventory records, and load the packed customer orders at the outbound decks. All these activities can be classified into four flows [5,6]: Flow 1 (receiving–cross-docking–shipping), Flow 2 (receiving–reserve area–shipping), Flow 3 (receiving–reserve area–forward area–shipping), and Flow 4 (receiving–forward area–shipping). These warehouse areas, flows, and activities are also visually introduced in Figure 1.

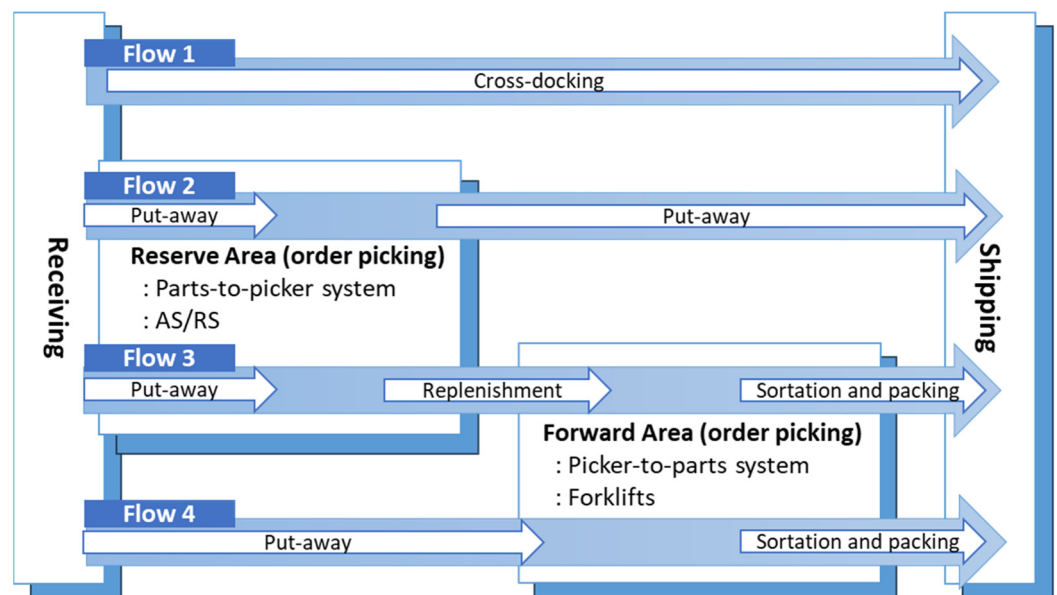


Figure 1. Warehouse areas, flows, and activities.

Among various warehouse activities, order picking is the most expensive activity in terms of EC and OT, and human- or automated machine-based order picking systems are used in a warehouse [6,9]. Among a variety of order-picking systems, two typical order-picking systems are (i) parts-to-picker and (ii) picker-to-parts systems. More specifically, an automated storage/retrieval system (AS/RS) is typically used for a parts-to-picker system, and forklifts can be used for all warehouse areas, including a picker-to-parts system. Thus, we can focus on the activities of AS/RS and forklifts in picker-to-part and part-to-picker systems to investigate EC and OT for warehouse operations.

A reserve area is usually occupied by parts-to-picker systems such as AS/RS. AS/RS uses various computer-controlled systems to automatically store and retrieve unit loads and can store and retrieve unit loads. The movement and travel time of the AS/RS crane or storage and retrieval (S/R) machine and picking time can directly decide AS/RS EC

and OT [10,11]. Different types of AS/RS show different energy effectiveness in warehouse systems [12–15]. Various AS/RS types can be recognized in the warehouse industry according to the S/R machines, handling, and rack properties in the system. Among different types of AS/RS, autonomous vehicle storage and retrieval systems (AVS/RS) have been broadly considered in the literature since these systems provide desirable flexibility by changing the number of vehicles to deal with the fluctuation in warehouse demand [7]. Besides, different AVS/RS designs such as shuttle-based storage and retrieval systems (SBS/RS) have been studied in the literature [8]. A basic AS/RS includes single-deep stationary racks in which S/R machines can directly store or retrieve unit loads. In some cases, a part of a unit load is considered for which a person can stand on an S/R machine to retrieve the required number of SKUs from the rack storage location. AS/RS can also bring the unit loads at the input/output (I/O) point by aisle-bound S/R machines, and pickers take the required number of SKUs; then, unneeded SKUs are returned to the storage location. A typical AS/RS handles one unit load (usually, in pallet size) at a time by a single shuttle on one S/R machine; an S/R machine is not able to change its aisle (aisle-captive type). For our study, this general type of AS/RS is considered since it is widely used.

Generally, a forward area is used for supporting order-picking activities and for storing fast-moving items that do not require a large amount of space in racks or on a floor [5,16]. Typically, a forward area is occupied by a picker-to-part system, where order picking equipment or people drive or walk along the aisles to pick items. Activities of a picker-to-part system can be classified into two types: low-level and high-level pickings. For low-level pickings, order pickers pick items from storage racks and bins while picking items from high storage racks for high-level pickings [6]. Since forklifts are typically used for order-picking activities, studies of forklifts will play a key role in EC and OT analysis in a warehouse forward area [17]. In addition, more than 60% of forklifts are powered by electricity, and therefore, the research focus needs to be on electric forklifts rather than on propane or diesel forklifts [9]. We also consider only electric forklifts in this study.

Forklifts and AS/RS are the most typical equipment and tools for warehouse forward and reserve areas, and their performance in terms of EC and OT is not independent of each other. This interdependency is observed when loads are handled by forklifts or other material handling equipment at AS/RS I/O points from a reserve area to other warehouse areas [18]. Flow 3 in Figure 1 shows this interdependency more specifically; Flow 3 accounts for a large material proportion, and the unit loads are always needed to replenish the picker-to-parts system in a forward area. This fact suggests that the parts-to-picker (reserve area) and picker-to-parts (forward area) systems influence each other in affecting EC and OT. For example, a delay in the parts-to-picker system can cause a subsequent delay in the picker-to-parts system, and forklift issues in the picker-to-parts system can result in another issue in the parts-to-picker system. Thus, a comprehensive analysis to identify significant factors and their interactions in both parts-to-picker (reserve area) and picker-to-parts systems (forward area) needs to be conducted.

Since interdependency between parts-to-picker and picker-to-parts systems can be observed at AS/RS I/O points, it is necessary to analyze the direct effects of buffer capacity (that is, the number of designed AS/RS I/O points) on EC and OT. A variety of factors including order size and the number of forklifts and S/R machines are also crucial in investigating EC and OT for both warehouse areas, simultaneously. Moreover, other warehouse activities such as cross-docking, put-away, and replenishment under different warehouse flows are also related to both picker-to-parts and parts-to-picker systems in affecting EC and OT. Thus, warehouse flow rates, which reflect different proportions among the four warehouse activities in Figure 1, are also required to be studied when we consider EC and OT. Overall, we can consider the following five important factors: (i) the number of forklifts, (ii) the number of S/R machines, (iii) the I/O buffer capacity of the AS/RS, (iv) the order size, and (v) the warehouse flow rate.

The number of energy-aware warehouse studies has increased in the recent literature, and energy saving of material handling equipment has been receiving as much attention

as other energy-aware warehouse topics such as building, lighting, and HVAC [2,4]. A comprehensive literature review of the EC of material handling equipment was provided in a survey by the study in [19]. The analysis of this review shows that the analytical and simulation methodologies have been considered much more than the methodologies supported by empirical data [10]. In some cases, mathematical optimization models may cause significant errors in interpreting the performance of warehouse systems since they usually use a limited number of deterministic factors and assumptions; moreover, they may not be able to handle a complex warehouse system and its changes over time. For example, the forklift EC significantly depends on load weights, and the weights may vary during forklift operations over time. Therefore, a simulation approach, which considers the changes in warehouse effective factors over time, can represent a better warehouse state for warehouse enterprises to make decisions in minimizing EC while responding to customer orders on time. Most current studies, however, have focused on mathematical models to determine the scheduling of forklift battery charging in making picker-to-parts systems sustainable; conversely, only a few studies have considered the energy-aware picker-to-parts systems by simulation as presented in Table 1. One example is the work of [20], who designed a simulation model to compare electric and fuel forklifts in terms of GHG for inbound warehouse activities. The results recommend using electric forklifts instead of fuel forklifts for the low- to medium-weight SKUs. The study in [21] also investigates replenishment and order-picking activities to minimize travel time and cost by simulation and a mathematical model. The proposed simulation uses the Dijkstra algorithm to address the forklift routing problem. The simulation analysis of the study also shows that EC reduction is significantly affected by the warehouse layout, operations, and material handling equipment. The advantages of simulation over mathematical models are described for warehouses in Table 1; most studies have broadly taken the same advantages in analyzing the parts-to-picker systems (AS/RS types). Table 1 shows that most simulation studies have been conducted either in a parts-to-picker system or in a picker-to-part system. We can also see that most parts-to-picker system studies focus on AS/RS or their variants. These observations clearly show that there exists a lack of research investigating integrated warehouses considering both forward and reserve areas, including those with AS/RS and forklifts.

Table 1. Summary of the literature.

Reference	Forward Area (Picker-to-Parts)	Reserve Area (Parts-to-Picker)			Performance Measure(s)	Method(s) Used with Simulation
		AS/RS	AVS/RS	SBS/RS		
[22]			✓		Cycle time and utilization	Design of Experiments (DOE)
[23]			✓		Cycle time and waiting time	Analytical model
[24]			✓		Cost and throughput	DOE
[11]		✓			Cycle time and EC	-
[25]		✓			GHG emissions	-
[26]		✓			Cycle time and EC	Mathematical model and large neighborhood search
[20]	✓				GHG emissions	-
[27]			✓		Travel time and cycle time	Analytical model
[28]				✓	Cycle time and throughput	DOE
[29]				✓	Cycle time and throughput	DOE
[21]	✓				Travel time and cost	Mathematical model and Dijkstra algorithm
[30]			✓		EC and energy recovering	-
[31]				✓	Throughput	Analytical model
[32]		✓			Travel time	DOE
[33]		✓			Travel time	Analytical model
[8]				✓	Cycle time, energy regeneration, and EC	DOE

AS/RS energy efficiency has become crucial in recent years for warehouses in order for them to become sustainable in all design factors in recent years [34]. In other words, a warehouse can be more sustainable by controlling AS/RS from an energy-aware per-

spective [15]. In particular, warehouse sustainability can be guaranteed by considering the relationships between inventory management, warehouse management, AS/RS EC, and GHG emissions [25]. The authors of [25] propose an integrated simulation to investigate the relationship between inventory management and warehouse GHG emissions. The study shows that AS/RS GHG emissions are lower than the GHG emissions generated by wide/narrow-aisle warehouses. The study in [11] also applies simulation to study the picking time and EC when S/R machines of an AS/RS are in an idle state; the results suggest that the movements of S/R machines cause a decrease in picking time and an increase in EC when the storage assignment and replenishment are determined. The proposed model in [26] considers the effects of AS/RS rack shapes on EC with a simulation time-based model; the study presents hybrid constraint programming and a large neighborhood search. The simulation is also designed particularly for storage assignment and operation sequencing problems. The results of the study demonstrate that there is a notable relationship between EC and rack height. Moreover, the authors of [33] examine different I/O point policies for AS/RS in which conveyors are used for depth transportation. The study formulates a travel time model which is verified by simulation. In terms of travel time, the study results show that a mid-point elevation policy is more effective than other policies.

Different types of AS/RS are categorized as complex systems with dynamic factors, so most AS/RS studies have widely studied them with simulation approaches. Among different types of AS/RS, the autonomous vehicle storage and retrieval system (AVS/RS) has been broadly considered in the literature since this system provides desirable flexibility by changing the number of vehicles to deal with the fluctuation of warehouse demand. Moreover, different AVS/RS designs such as shuttle-based storage and retrieval systems (SBS/RS) have been studied in the literature. For example, the study of [23] uses simulation to verify an analytical model formulated based on an open queuing network approach for an AVS/RS. The study formulates the model to examine the cycle time and waiting times of tote movements with a captive-tier configuration. The results show that the average cycle time and waiting time could be reduced by applying the proposed model. The authors of [27] use an analytical model and simulation to study the travel time/distance and cycle time for single- and dual-command cycles of an AVS/RS. The proposed model is validated by simulation, and different layout configurations with multiple deep storage lanes are considered for a real warehouse. The approach in [30] presents a simulation model for the travel time and EC to examine and compare the energy balance and recovery measurements of an AVS/RS. The results of the study indicate that around 28% of EC could be recovered in the AVS/RS. The research in [31] applies simulation to verify a travel time model formulated for a tier-to-tier SBS/RS under a dual command. The study investigates the SBS/RS performance by alternative factors such as the physical configuration, vehicle acceleration/deceleration (A/D) rate and velocity, and shuttle operational probability.

If a single S/R machine is considered for AS/RS, the basic physics laws to calculate EC and power of S/R machines can be applied to forklifts and S/R machines. Then, the power and EC of simulated S/R machines and forklifts can be measured by previous studies [8,12,35–37]. For the travel time models, the study of [38] can be referred to. Also, most existing studies do not utilize real data on EC and the movements of forklifts. To address this lack of studies, we use (i) power data on forklift battery chargers collected from experiments and (ii) forklift power and travel data provided by a forklift manufacturer [2,39]. From these datasets, this research can perform a more realistic EC and OT analysis.

Design of experiments (DOE) is a robust method and has been extensively used for simulation results in the literature to identify significant factors affecting the various measures of warehouse performance. Researchers have also applied this method to determine the relationships between different warehouse factors over time from the simulation results as shown in Table 1. The authors of [32] use a simulation-based experimental design to address the effects of various physical designs, storage policies, and environmental

factors on the travel time of a single-crane multi-aisle AS/RS with a single command cycle. The study shows that the small number of aisles decreases the advantages of a cross-aisle full-turnover storage policy while increasing the benefits of a random storage policy. The study of [24] presents a simulation-based DOE to identify key factors between AVS/RS tier-captive and tier-to-tier configurations. The proposed DOE examines the effects of AVS/RS factors on different performance measures such as cost. The analysis of the study also shows that the cost could be minimized by decreasing the number of aisles and increasing the aisle length. The research in [22] uses a simulation-based DOE to find significant factors affecting the performance of AVS/RS in terms of average storage and retrieval cycle time, and the average utilization of lifts and vehicles. The study defines different scenarios for lifts and vehicles with various arrival rates. The results show that the combination of the highest factor levels could present the best scenario for the AVS/RS system. The author of [8] also applies a simulation-based experimental design to recognize significant factors influencing the pre-defined performance measures of a shuttle-based storage and retrieval system (SBS/RS). The study uses a full factorial design to investigate the effects of velocity, acceleration, and the number of bays and tiers on the average cycle time, energy regeneration, and EC. The author of [28] proposes a DOE for an SBS/RS to find an optimized scenario for single and dual command cycle times and throughput. The factors considered in the study include the number of bays and tiers, shuttle A/D rate and velocity, and elevator A/D rate and velocity. The results exhibit that the best scenarios belong to the small number of bays and tiers. The study in [29] also applies a similar DOE with the same performance measures and different design factors such as the number of bays and minimum warehouse volume for an SBS/RS. The results of the study indicate that the SBS/RS system operates more efficiently with high racks and a small number of tiers.

As shown previously, both warehouse forward and reserve areas need to be studied together since they are interconnected in evaluating EC and OT. Thus, we designed an energy-aware simulation model in SIMIO software (version 15) and integrated warehouse forward and reserve areas by considering AS/RS, forklifts, and storage racks. In this research, we also apply real power and movement data to support the proposed energy-aware simulation of forklifts and S/R machines, and this endeavor will contribute to filling the lack of real-power-based simulation studies in the literature. In order to consider various warehouse activities such as cross-docking, replenishment, and put-away under various warehouse flows, five factors are considered in DOE: (i) the number of forklifts, (ii) the number of S/R machines, (iii) the I/O buffer capacity of the AS/RS, (iv) the order size, and (v) the flow rate. The flow rate factor is defined based on the proportion of loads on warehouse flows moving through forward and reserve areas. Factorial design is used for DOE to identify the significant factor(s) influencing EC and OT from the simulation results. DOE analyses will provide a comprehensive investigation for warehouse decision-makers to improve EC and OT in the warehouse reserve and forward areas together. Thus, this study will help industrial practitioners reduce and save EC and OT in warehouse operations. The results from this study can also encourage and benefit relevant warehouse research studies by providing real EC and movement data from forklifts and battery chargers. The rest of this paper is organized as follows. Section 3 presents relevant models for warehouse simulation as well as EC. DOE results are provided in Section 4, and we discuss the results with potential future research work in Section 5.

3. Models for Simulating Warehouse Energy

To evaluate EC and OT during simulation runs, we need models for the computing power and travel time of material handling equipment. Thus, in this section, we provide models for estimating power and travel time to be used for forklifts and S/R machines in simulation models. Then, the simulation model is also introduced.

3.1. Travel Time Models for Forklifts and S/R Machines

EC is calculated as power used for a certain amount of time. When the EC for forklifts and S/R machines is calculated, operational factors such as the A/D rate and velocity are needed for evaluating the travel time. For that, the study in [38] can be applied, and the EC of forklifts and S/R machines can be estimated based on real forklift power data provided by [2,39]. Following the information and data by [2,39], relevant factors and parameters are defined to explain the relationships among the forklift A/D rate, velocity, and travel time: $a = A/D$ rate (m/s^2), $v_t =$ velocity at time t (m/s), $v_{max} =$ maximum velocity (m/s), $t_{peak} =$ time duration needed to reach peak velocity (second), $d_{peak} =$ travel distance needed to reach v_{max} (meter), $T =$ total travel time (second), and $d_T =$ total travel distance (meter). The weight of the forklift or S/R machine is assumed to be 5971 kg.

Then, two possible travel scenarios can be considered. In the first scenario, a forklift or S/R machine cannot move as far as d_{peak} or reach v_{max} while it can reach v_{max} in the second scenario. Equations (1) and (3) calculate the forklift velocity v_t at time t based on the A/D rate a and v_{max} for the first and second scenarios, respectively. These two scenarios are visually shown in Figure 2. Moreover, Equations (2) and (4) measure the total travel distance d_T according to v_t for the first and second scenarios, respectively. Equation (5) calculates d_{peak} based on v_t .

$$v_t = \begin{cases} a \cdot t & t \in [0, t_{peak}] \\ -a \cdot (t - T) & t \in [t_{peak}, T] \end{cases} \quad (1)$$

$$d_T = \int_0^T v_t \cdot dt = \frac{a}{4} \cdot T^2 \quad (2)$$

$$v_t = \begin{cases} a \cdot t & t \in [0, t_{peak}] \\ v_{max} & t \in [t_{peak}, T - t_{peak}] \\ -a \cdot (t - T) & t \in [T - t_{peak}, T] \end{cases} \quad (3)$$

$$d_T = \int_0^T v_t \cdot dt = v_{max} \cdot T - \frac{v_{max}^2}{a} \quad (4)$$

$$d_{peak} = \int_0^{t_{peak}} v_t \cdot dt = \frac{v_{max}^2}{a} \quad (5)$$

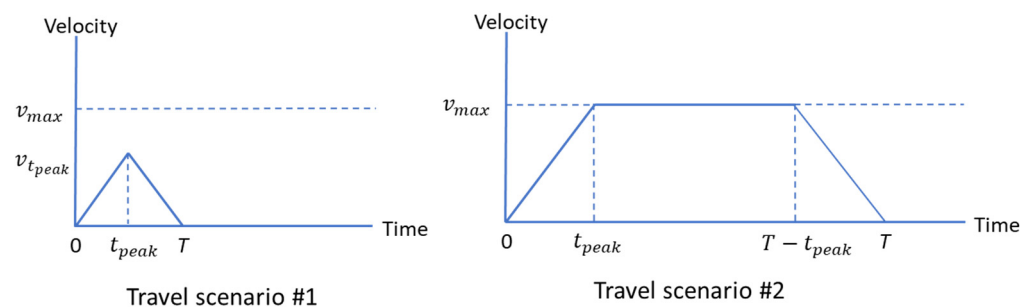


Figure 2. Two travel scenarios of forklifts and S/R machines.

For material handling equipment such as forklifts and S/R machines, horizontal and vertical movements are assumed when they travel from SKU i to j . Then, the A/D rate, velocity, and travel time of forklifts or S/R machines can be defined in various cases for both horizontal and vertical movements. Figure 3 illustrates the combination of the travel scenarios in the horizontal and vertical directions. According to Equations (2) and (4), Equations (6) and (7) also calculate horizontal and vertical travel times, respectively, for

which the following parameters are defined: $a^x = A/D$ rate in the horizontal direction (m/s^2), $a^y = A/D$ rate in the vertical direction (m/s^2), $v_{max}^x =$ maximum velocity in the horizontal direction (m/s), $v_{max}^y =$ maximum velocity in the vertical direction (m/s), $d_{peak}^x =$ travel distance needed to reach v_{max}^x , $d_{peak}^y =$ travel distance needed to reach v_{max}^y , $d_{i,j}^x =$ travel distance between SKU i and j in the horizontal direction (meter), $d_{i,j}^y =$ travel distance between SKU i and j in the vertical direction (meter), $t_{i,j}^x =$ travel time between SKU i and j in the horizontal direction (second), and $t_{i,j}^y =$ travel time between SKU i and j in the vertical direction (second).

$$t_{i,j}^x = \begin{cases} \sqrt{\frac{4 \cdot d_{i,j}^x}{a^x}} & 0 \leq d_{i,j}^x \leq d_{peak}^x \\ \frac{d_{i,j}^x}{v_{max}^x} + \frac{v_{max}^x}{a^x} & d_{peak}^x \leq d_{i,j}^x \end{cases} \quad (6)$$

$$t_{i,j}^y = \begin{cases} \sqrt{\frac{4 \cdot d_{i,j}^y}{a^y}} & 0 \leq d_{i,j}^y \leq d_{peak}^y \\ \frac{d_{i,j}^y}{v_{max}^y} + \frac{v_{max}^y}{a^y} & d_{peak}^y \leq d_{i,j}^y \end{cases} \quad (7)$$

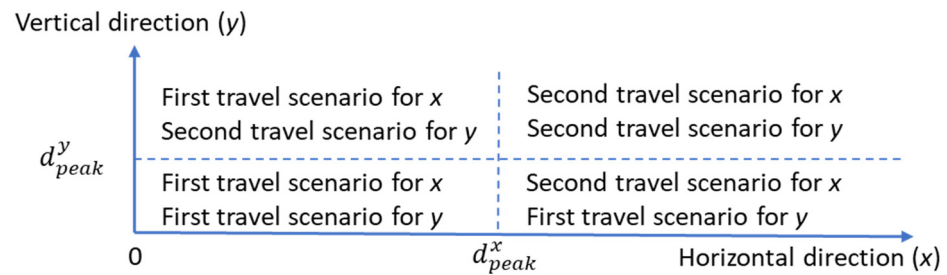


Figure 3. Four travel scenarios regarding horizontal and vertical movements.

From the available data, we can estimate the following parameters. As shown in Figure 4, the average A/D rate for 8.73 s is $a^x = 0.409 m/s^2$, and from 8.74 to 15.41 s, the maximum constant velocity of $v_{max}^x = 3.576 m/s$ can be observed with the horizontal direction of a forklift. Then, $t_{i,j}^x$ can be evaluated with Equation (6) given a^x , v_{max}^x , and the distance between SKUs i and j in the horizontal direction ($d_{i,j}^x$).

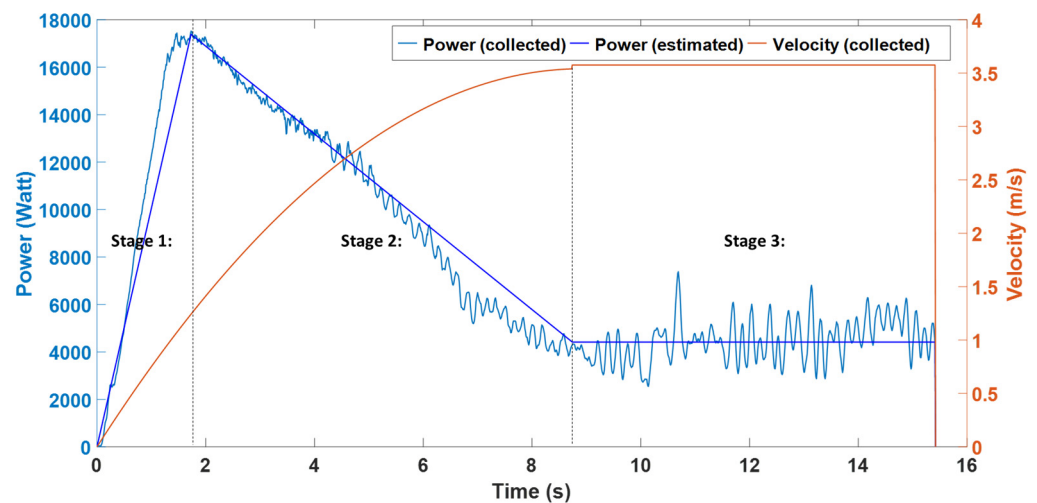


Figure 4. Collected and estimated power and velocity for horizontal movements.

The vertical movement velocity and power of the forklift is presented in Figure 5. The forklift lifts the load with the constant velocity of $v^y = 1.162 m/s$ by its carriage for $t_v = 4.97 s$.

While we assume that the forklift has an A/D rate in the horizontal direction, it seems to keep a constant velocity with no A/D rate in the vertical direction. Thus, $a^y = 0 \text{ m/s}^2$, and we cannot use Equation (7) to measure $t_{i,j}^y$ according to the distance between SKUs i and j in the vertical direction ($d_{i,j}^y$). Equation (8), which is formulated instead of Equation (7), measures $t_{i,j}^y$ according to $d_{i,j}^y$, $t_v = 4.97 \text{ s}$, and the two vertical constant velocities ($v^y = 1.162 \text{ m/s}$) [2].

$$t_{i,j}^y = \begin{cases} \frac{d_{i,j}^y}{v_1^y} & 0 \leq d_{i,j}^y \leq v_1^y \cdot t_v \\ t_v + \frac{d_{i,j}^y - v_1^y \cdot t_v}{v_2^y} & v_1^y \cdot t_v \leq d_{i,j}^y \end{cases} \quad (8)$$

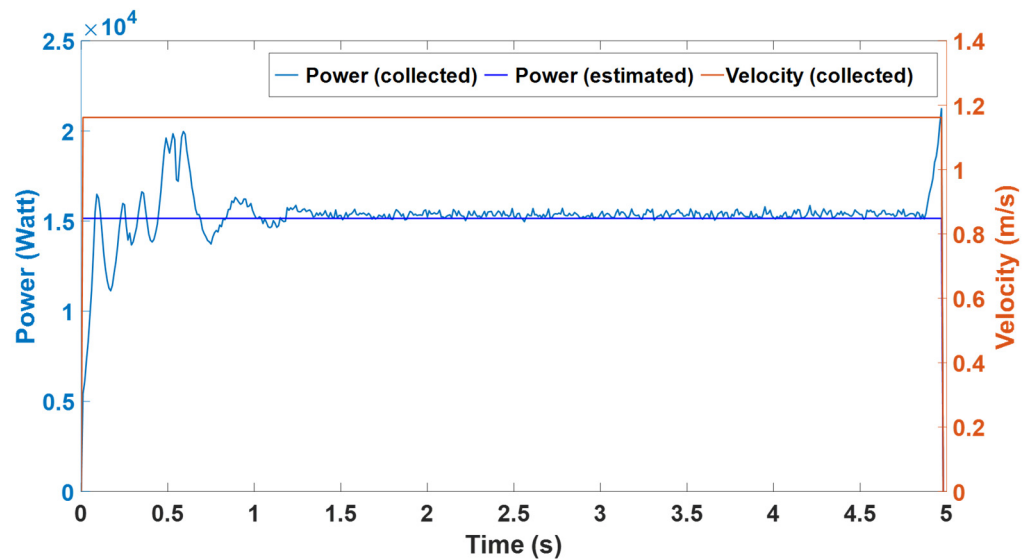


Figure 5. Collected and estimated power and velocity for vertical movements.

3.2. Power Models for Forklifts (S/R Machines) and Battery Chargers

We first model the power of forklifts and S/R machines for horizontal and vertical movements, respectively, and then provide a model for the power of forklifts' battery chargers. These models will be used for simulation scenarios by varying movement times and weights of loads in evaluating EC and OT.

3.2.1. Horizontal Movement Power Models

To model the power of forklifts or S/R machines in horizontal movement, we used the power data of a forklift in the time resolution of 0.01 s provided by [39] (see Figure 4). According to the available data, the power of forklifts in a horizontal movement can be modeled in three stages. A forklift (S/R machine) accelerates in Stages 1 and 2 and remains at a constant maximum velocity in Stage 3. Stage 1 of the model begins with the power of $p_0 = 0$ Watts and ends at a peak power p_1 with the velocity of $v_p = 1.243 \text{ m/s}$; afterwards, the power declines from p_1 to a constant power p_2 in Stage 2. Finally, the power remains constant with the amount of p_2 in Stage 3. Two linear power equations are applied to model the power of Stages 1 and 2, and the constant power of p_2 is considered for Stage 3. Stages 1 and 2 take 1.73 and 7.01 s, respectively, and the rest of the movement time stays at Stage 3. From these models, we can estimate power forklifts and S/R machines as a function of movement time. Then, we apply the horizontal power model in [37] for the simulation using the available data and estimate the relevant parameters as follows:

$$G = (m_f + m_l) \cdot g \quad (9)$$

$$F = \begin{cases} G \cdot \mu_1 + \frac{G}{g} \cdot a_p \cdot k & \text{if } t = t_1 \\ G \cdot \mu_2 & \text{if } t = t_2 \end{cases} \quad (10)$$

$$p_1 = \frac{F \cdot v_p}{\eta} \quad (11)$$

$$p_2 = \frac{F \cdot v_{max}}{\eta} \quad (12)$$

$$p_h = \begin{cases} \frac{p_1}{t_1} \cdot t & \text{if } t \leq t_1 \\ \frac{p_2 - p_1}{t_2 - t_1} \cdot (t - t_1) + p_1 & \text{if } t_1 \leq t \leq t_2 \\ p_2 & \text{otherwise} \end{cases} \quad (13)$$

where G = force of gravity ($N = \text{kg} \times \text{m/s}^2$), m_f = forklift mass (kg), m_l = load mass (kg), g = gravity acceleration $\approx 9.8 \text{ m/s}^2$, F = traction force ($N = \text{kg} \times \text{m/s}^2$), μ_1 = coefficient of resistance including rolling and aerodynamics for forklifts with acceleration in Stage 1 = 0.140, a_p = acceleration at peak power = 0.64 m/s^2 , k = rotating mass coefficient = 1.150, μ_2 = coefficient of resistance including rolling and aerodynamics for forklifts with constant velocity in Stage 3 = 0.019, p_1 = peak power in Stage 1 (Watt), v_p = velocity at peak power = 1.243 m/sec , η = efficiency of mechanical systems (0.9 for motors, pumps, etc.), p_2 = constant power in Stage 3 (Watt), v_{max} = constant maximum velocity in Stage 3 (m/s), p_h = power for horizontal movement (Watts = $\text{kg} \times \text{m}^2/\text{s}^3$), t_1 = start time of Stage 2 = 1.73 s, t = time passed in horizontal movement (s), and t_2 = start time of Stage 3 = 8.74 s.

Equations (9) and (10) calculate the gravity and traction forces, respectively. Equations (11) and (12) measure the peak power and constant power for the horizontal forklift movement, respectively. Equation (13) also calculates the forklift power in the horizontal movement from Equations (11) and (12). To validate this model, we solved the proposed model based on the maximum velocity ($v_{max} = 3.576 \text{ m/s}$) and forklift weight ($m_f + m_l = 5971 \text{ kg}$) and observed that there was a 0.22% power difference between the fitted model and the provided forklift energy data. Figure 4 also shows how the modeled power closely fits the real (collected) power data. For simulation, m_l values will be varied, and power will be evaluated for each load/pallet.

3.2.2. Vertical Movement Power Models

According to the available forklift energy and movement data, the forklift uses a carriage in the lifting operation/vertical movement. The data in Figure 5 show that the velocity of the carriage movement is almost constant. Hence, we model the power in such a way that each forklift spends the entire time of vertical movement with a constant velocity (v). According to the available data [39] and a model proposed by [37], we formulated a vertical power model as Equations (14) and (15); these equations measure the gravity force and forklift power in a vertical movement, respectively.

$$G = (m_c + m_l) \times g \quad (14)$$

$$p_v = \frac{k \times G \times v_v}{\eta} \quad (15)$$

where m_c = carriage mass of the carriage (kg), m_l = load mass (kg), g = gravity acceleration $\approx 9.8 \text{ m/s}^2$, k = counterweight coefficient = 2.2 (=1 if the counterweight is not applied), v_v = constant vertical velocity (m/s), η = efficiency of mechanical systems (0.9 for motors, pumps, etc.), G = force of gravity ($N = \text{kg} \times \text{m/s}^2$), and p_v = power for vertical movement (Watts = $\text{kg} \times \text{m}^2/\text{s}^3$).

Since the proposed vertical model is formulated based on the data from the forklift manufacturer, it is necessary to examine and compare the model results with the forklift data [39]. We set $v = 1.162$ m/s according to the data and assume that $m_c + m_l = 544.31$ kg as the input parameters of the model. The results show that the modeled power properly fits the data, and there is a 2.08% difference between them as in Figure 5. For simulation, m_l values will be varied, and power will be evaluated for each load/pallet.

3.2.3. Battery Charger Power Model

To model the battery charging power, we collected real data from a charger used for a lead-acid battery with 38 V, 1105 Ah, and 18 cells as in Figure 6. We studied this battery type since the battery specifications are close to the forklift battery considered in this research. The collected data show that this lead-acid battery is charged with three stages: in Stage 1, a constant-current charge provides the main part of the charge, in Stage 2, a topping charge saturates the charge of the battery, and in Stage 3, a float charge is applied to help the battery not to be self-discharged. According to the data, 2300 s and 6260 s out of the charging time are assigned to Stages 1 and 2, respectively, and the remaining charging time is dedicated to Stage 3. The amount of power during Stages 1 and 3 is also assumed to be constant in the model. Thus, the averages of power in the relevant stages of the real data are measured and used as the constant powers of the model. We also used the curve fitting tool to model the power of Stage 2. The notations and power formulations are provided in Equation (16).

$$p_{ch} = \begin{cases} p_1 = 11099.21 & \text{if } t \leq t_1 \\ 10603 - 1.559 \times (t - t_1) + 0.000105 \times (t - t_1)^2 & \text{if } t_1 < t \leq t_2 \\ p_2 = 4821.68 & \text{otherwise} \end{cases} \quad (16)$$

where t_1 = start time of topping charge (Stage 2) = 2300 s, t_2 = start time of float charge (Stage 3) = 9680 s, t = time passed in charging (s), p_1 = average of power in Stage 1 = 11,099 Watts, p_2 = average of power in Stage 3 = 4822 Watts, and p_{ch} = power of the charger (Watt).

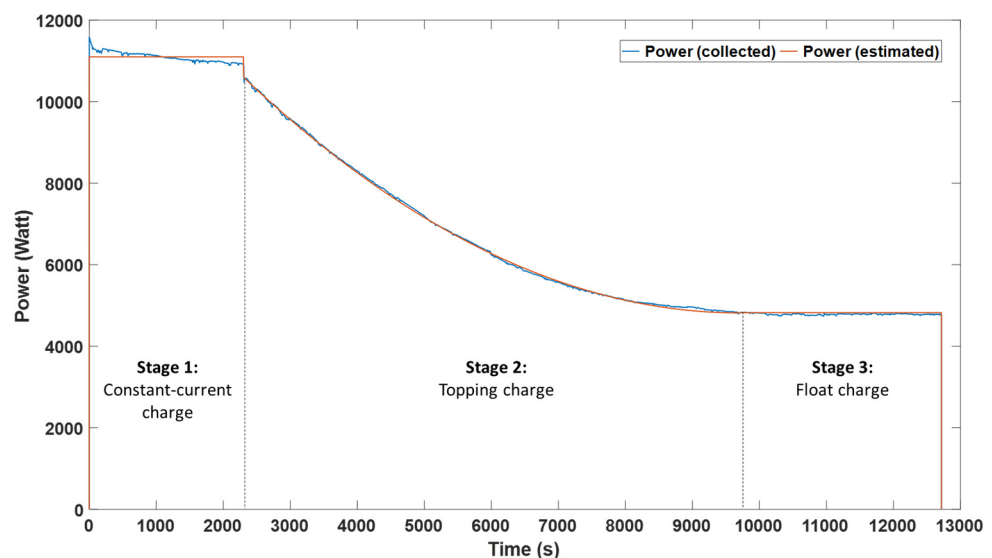


Figure 6. Collected and estimated power of a forklift battery charger.

Equation (16) provides the estimated power of the charger. The results of the proposed model show that there is a 0.01% difference between the power calculated from the model and the real data. Also, Figure 6 illustrates that the modeled power closely fits the real power data. The proposed model in Equation (16) will be used to model the power of forklift battery chargers for simulations. Regarding the amounts of $t_{i,j}^x$ and $t_{i,j}^y$, we can

measure and calculate the forklift and S/R machine EC in the horizontal and vertical directions from the available forklift data for simulation scenarios [39].

3.3. Simulation Models for Warehouses

There exist interactions between picker-to-parts (forward) and parts-to-picker (reserve) systems in a warehouse, and these interactions have effects on EC and OT. Thus, we built and simulated a warehouse that consists of the integrated picker-to-parts (forward) and parts-to-picker system (reserve) by considering the movements of forklifts and S/R machines to analyze EC and OT. This warehouse is 460 feet (≈ 140.2 m) long and 265 feet (≈ 80.8) wide, and therefore, its area is 121,900 ft² ($\approx 11,325$ m²) as illustrated in Figure 7. This simulation model connects the AS/RS in a parts-to-picker system to the picker-to-parts systems through AS/RS I/O points, where forklifts receive the unit-loads (pallets) from the AS/RS to make shipments or replenish the picker-to-parts system in the forward area.

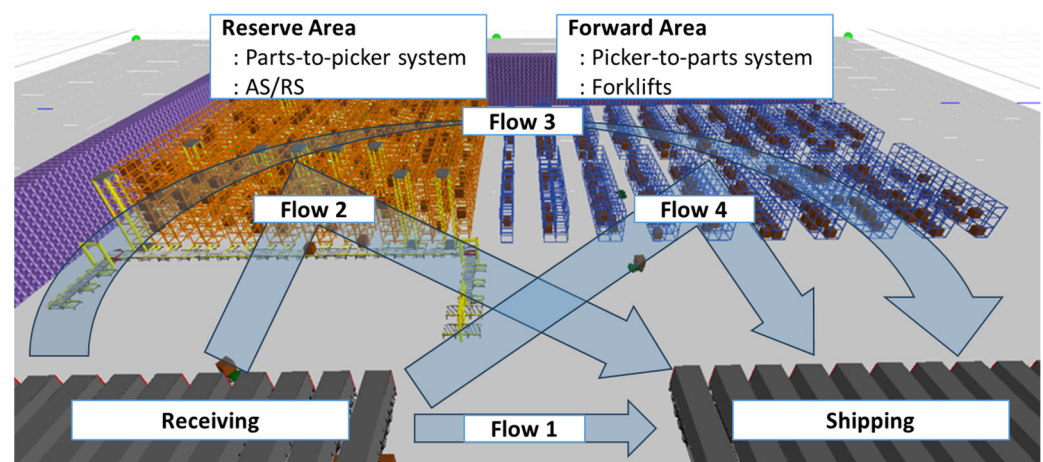


Figure 7. Major warehouse areas and flows on a simulation model.

The simulation of this integrated warehouse was modeled with SIMIO software (version 15) to examine EC and OT. Table 2 lists the specifications of the picker-to-parts system (forward area) and the part-to-picker system (AS/RS) designed in our simulation.

In the simulation, EC measurements of forklifts and battery chargers were performed over time according to the power models presented in Sections 3.1 and 3.2. To apply these models in the simulation model and generate outputs as Excel files, we used various logic processes in SIMIO. More specifically, the outputs of the simulation from SIMIO are (i) the location names of forklifts at the time, (ii) the description status of forklifts at the time, (iii) the loading status of forklifts at the time (=1 of loaded; 0 otherwise), (iv) the load mass of forklifts at the time (kg), (v) the location X-coordinate of forklifts at the time (meters), (vi) the location Y-coordinate of forklifts at the time (meters), (vii) the location Z-coordinate of forklifts at the time (meters), (viii) the current time, (ix) the power of forklifts and forklift battery chargers at the time (Watt), and (x) the EC of forklifts and forklift battery chargers (Watt·sec). Then, we imported the outputs of SIMIO (Excel files) in MATLAB to generate the power time series of forklifts, S/R machines, and forklift battery chargers. For the simulation processes for generating time series, the study in [40] can be referred to.

We assume that each forklift or S/R machine is capable of picking a maximum of 45 SKUs ($C^f = 45$) with similar dimensions in each tour [41]. Also, the mass capacity of forklifts or S/R machines is considered as 1360 kg. The average time of a battery fast charging (θ) is assumed to be 20 min [42]. We collected real power data for 20 min from a charger of a lead-acid battery with 38 V and 1105 Ah, and 18 cells as shown in Section 3.2; accordingly, we assumed that the maximum EC of forklift between two consecutive fast chargings EC_{max} is 3.73 kWh.

Table 2. Parameters of the simulated warehouse.

Area	Equipment	Specification
Forward Area (Picker-to-Parts)	Length	243 ft (\approx 74.1 m)
	Width	159 ft (\approx 48.5 m)
	Height	18 ft (\approx 5.5 m)
	Number of forklifts	1 or 5
	Number of battery chargers	3
	Number of storage locations	1296
	Number of bays per rack	12
	Number of tiers per rack	3
	Number of racks	18
	Length of rack	72 ft (\approx 21.9 m)
	Width of rack	6 ft (\approx 1.8 m)
	Height of rack	18 ft (\approx 5.5 m)
	Number of aisles	18
	Length of aisle	72 ft (\approx 21.9 m)
Width of aisle	15 ft (\approx 4.6 m)	
Reserve Area (Parts-to-Picker)	Length	168 ft (\approx 51.2 m)
	Width	162 ft (\approx 49.4 m)
	Height	36 ft (\approx 11.0 m)
	Number of S/R machines	4 or 9
	Number of I/O points	2 or 6
	Number of storage locations	3000
	Number of bays per rack	28
	Number of tiers per rack	6
	Number of racks	18
	Length of rack	168 ft (\approx 51.2 m)
	Width of rack	6 ft (\approx 1.8 m)
	Height of rack	36 ft (\approx 11.0 m)
	Number of aisles	4 or 9
	Length of aisle	168 ft (\approx 51.2 m)
Width of aisle	6 ft	

The following assumptions are considered for the DOE of the integrated picker-to-parts and parts-to-picker system. We set the simulation run time (24 h) and the number of orders (100 orders) as two criteria to terminate the simulations of EC and OT, respectively. We ran each DOE scenario with three replications. A 4 h warm-up time was set for each simulation run. Each S/R machine or forklift can process two types of transaction/task: storage transactions (reach pallets to racks) and retrieval transactions (pick up pallets from racks). S/R machines and forklifts process the transactions based on the first-in-first-out (FIFO) rule and cannot be interrupted during a transaction. The closest forklift is assigned to a transaction when needed; all other default settings are accepted for detailed operations and routings of forklifts and S/R machines. S/R machines and forklifts stay at their current locations in an idle state. S/R machines and forklifts move pallets to available storage locations, randomly. The order size is assumed to be the number of pallets, and each S/R machine or forklift can load/unload one pallet at a time. The interarrival time of pallets from the inbound docks is exponentially distributed with an average of 0.01 h. S/R machines and forklifts move/store pallets to available storage locations, randomly. Pallet weight is randomly generated from the uniform distribution with $U[500, 1500]$ in kg. The storage time in AS/RS is randomly generated from the uniform distribution of $U[8, 16]$ h. The storage time in the picker-to-parts system is uniformly generated as $U[4, 8]$ h. The processing time of cross-docking is assumed to be one hour. Order interarrival time is exponentially distributed with an average of 0.05 h. Order due dates are randomly distributed from the uniform distribution $U[4, 6]$ in hours. The load capacity of all S/R machines and forklifts is 1500 kg. The acceleration and maximum velocity of S/R machines and forklifts are assumed to be 0.64 m/s^2 and 3.576 m/s , respectively, in horizontal movements. The constant velocity of S/R machines and forklifts is assumed to

be 1.162 m/s in vertical movements. The weight of an S/R machine (shuttle) or a forklift carriage is assumed to be 544.31 kg. The weight of an AS/RS crane or a forklift is assumed to be 4471 kg. The same battery capacity is assumed for all forklifts (≈ 25 kWh). An empty forklift battery needs 12,715 s to be fully charged. Forklifts remain idle during battery charging. The buffer capacity of AS/RS output points located between the reserve and the forward areas is examined and controlled in DOE. Each aisle of AS/RS has a one-pallet buffer capacity at its input point.

Figure 8 illustrates an example of the simulated power of forklifts, battery chargers, and S/R machines over a 24 h run. More specifically, the warehouse simulation provides the time series electrical loads of S/R machines, forklifts, and battery chargers. While the forklift EC is measured to determine the battery charging scheduling, it does not contribute to the total warehouse EC since the EC of forklifts is considered only through the EC of forklift battery chargers.

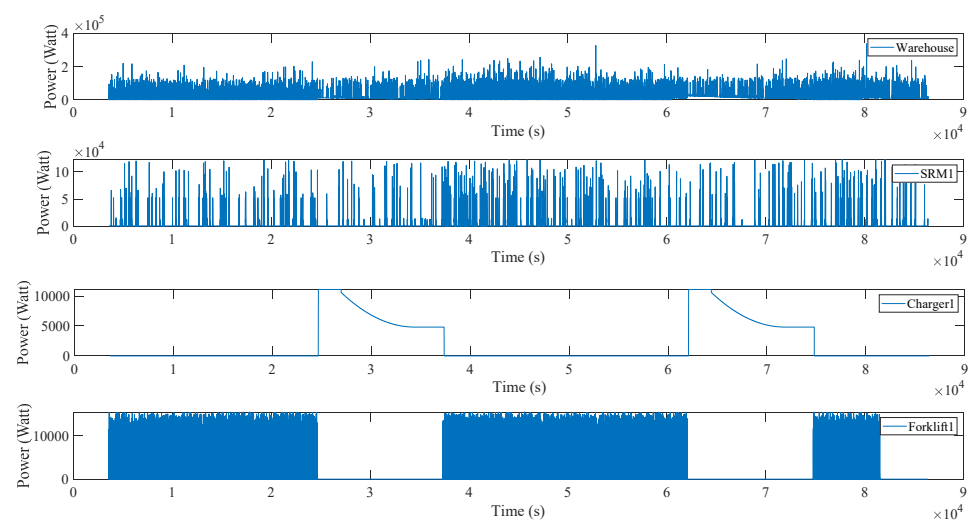


Figure 8. Simulated power of a warehouse, S/R machines, battery chargers, and forklifts for 24 h.

4. Results with Experimental Design

A 2^5 factorial design was conducted for EC and OT, separately, to examine the main effects and interaction effects of five important factors: the number of forklifts (x_1), the number of S/R machines (x_2), the I/O buffer capacity of the AS/RS (number of pallets) (x_3), the order size (number of pallets) (x_4), and the flow rate (x_5). In DOE, x_5 represents the proportion of pallets that are moved through Flows 1, 2, 3, and 4 as presented in Sections 1 and 2. In more detail, Table 3 provides the values of each factor with two experimental levels. For example, the value of x_3 is selected from the discrete uniform distributions $U\{2, 4\}$ and $U\{4, 6\}$ with the low and high levels of the experiment, respectively. In other words, either two or four pallets can be randomly selected with the same probability as x_3 with the low level, and four or six pallets can be randomly selected with the same probability as x_3 with the high level. Also, the low level of x_5 in DOE is defined as the proportions of 2, 1, 1, and 2 (33.3%, 16.5%, 16.5%, and 33.3%) for Flows 1, 2, 3, and 4, respectively. The different configurations of x_5 are designed with the high level, which is the proportions of 1, 2, 2, and 1 (16.5%, 33.3%, 33.3%, and 16.5%) for Flows 1, 2, 3, and 4, respectively.

Table 3. DOE for integrated picker-to-parts and parts-to-picker systems.

Factors	Levels	
	Low Level (−1)	High Level (1)
Number of forklifts (x_1)	1	5
Number of S/R machines (x_2)	4	9
I/O buffer capacity of AS/RS (number of pallets) (x_3)	Discrete U{2, 4}	Discrete U{4, 6}
Order size (number of pallets) (x_4)	Discrete U{1, 2}	Discrete U{2, 3}
Flow rate (x_5)	Flows 1 and 4 (67%) & Flows 2 and 3 (33%)	Flow 1 and 4 (33%) and Flows 2 and 3 (67%)

4.1. DOE for the EC of Integrated Energy-Aware Picker-to-Parts and Parts-to-Picker Systems

Simulation results for EC based on a 2^5 factorial design are reported in Table 4; three replications are carried out for each treatment, and the average response is reported in the table. The analysis of variance (ANOVA) results of the factorial design are also provided in Table 5. Figure 9 shows the half-normal plot of effects on average EC.

Table 4. DOE results for the average EC of integrated picker-to-parts and parts-to-picker systems.

Scenarios	Factors and Levels					Average EC (kWh)
	x_1	x_2	x_3	x_4	x_5	
1	−1	−1	−1	1	1	246.21
2	−1	−1	−1	−1	−1	178.96
3	−1	−1	1	1	1	253.75
4	−1	1	1	1	1	288
5	−1	1	−1	1	1	284.52
6	−1	−1	1	−1	1	259.29
7	−1	1	−1	−1	1	286.06
8	−1	−1	−1	−1	1	257.08
9	−1	−1	1	1	−1	183.15
10	−1	−1	−1	1	−1	176.56
11	−1	1	1	−1	1	282.09
12	−1	−1	1	−1	−1	181.68
13	−1	1	1	1	−1	231.14
14	−1	1	1	−1	−1	231.48
15	−1	1	−1	−1	−1	226.9
16	−1	1	−1	1	−1	225.69
17	1	1	−1	−1	1	291.56
18	1	1	−1	1	−1	259.11
19	1	1	1	−1	−1	262.79
20	1	−1	−1	−1	1	275.46
21	1	−1	1	1	1	285.74
22	1	1	1	−1	1	312.42
23	1	−1	1	−1	1	284.55
24	1	−1	−1	−1	−1	203.25
25	1	1	−1	1	1	299.6
26	1	−1	−1	1	1	275.36
27	1	−1	1	−1	−1	209.14
28	1	−1	1	1	−1	205.06
29	1	−1	−1	1	−1	209.79
30	1	1	1	1	1	315.38
31	1	1	1	1	−1	274.42
32	1	1	−1	−1	−1	260.82

Table 5. ANOVA for the average EC of integrated picker-to-parts and parts-to-picker systems.

Source	DF	Adj SS	Adj MS	F-Value	p-Value
Model	31	153,282	4944.6	89.37	0
Linear	5	147,244	29,448.8	532.28	0
x_1	1	17,488	17,488.5	316.1	0
x_2	1	39,238	39,237.9	709.22	0
x_3	1	997	997.5	18.03	0
x_4	1	9	9.3	0.17	0.683
x_5	1	89,511	89,510.7	1617.89	0
Two-way interactions	10	4891	489.1	8.84	0
$x_1 \cdot x_2$	1	7	6.9	0.12	0.726
$x_1 \cdot x_3$	1	198	197.9	3.58	0.063
$x_1 \cdot x_4$	1	143	142.5	2.58	0.113
$x_1 \cdot x_5$	1	405	405.2	7.32	0.009
$x_2 \cdot x_3$	1	53	53	0.96	0.331
$x_2 \cdot x_4$	1	132	132.2	2.39	0.127
$x_2 \cdot x_5$	1	3847	3846.9	69.53	0
$x_3 \cdot x_4$	1	25	25.4	0.46	0.5
$x_3 \cdot x_5$	1	71	71.4	1.29	0.26
$x_4 \cdot x_5$	1	9	9.1	0.16	0.686
Three-way interactions	10	871	87.1	1.57	0.135
$x_1 \cdot x_2 \cdot x_3$	1	172	171.9	3.11	0.083
$x_1 \cdot x_2 \cdot x_4$	1	1	0.7	0.01	0.909
$x_1 \cdot x_2 \cdot x_5$	1	355	354.6	6.41	0.014
$x_1 \cdot x_3 \cdot x_4$	1	32	32.4	0.59	0.447
$x_1 \cdot x_3 \cdot x_5$	1	214	214	3.87	0.054
$x_1 \cdot x_4 \cdot x_5$	1	8	8.1	0.15	0.704
$x_2 \cdot x_3 \cdot x_4$	1	26	26.1	0.47	0.495
$x_2 \cdot x_3 \cdot x_5$	1	9	9.2	0.17	0.684
$x_2 \cdot x_4 \cdot x_5$	1	53	53.5	0.97	0.329
$x_3 \cdot x_4 \cdot x_5$	1	0	0.2	0	0.951
Four-way interactions	5	159	31.8	0.57	0.72
$x_1 \cdot x_2 \cdot x_3 \cdot x_4$	1	32	31.9	0.58	0.45
$x_1 \cdot x_2 \cdot x_3 \cdot x_5$	1	14	13.6	0.25	0.622
$x_1 \cdot x_2 \cdot x_4 \cdot x_5$	1	34	33.7	0.61	0.438
$x_1 \cdot x_3 \cdot x_4 \cdot x_5$	1	20	19.8	0.36	0.551
$x_2 \cdot x_3 \cdot x_4 \cdot x_5$	1	60	59.7	1.08	0.303
Five-way interactions	1	118	117.9	2.13	0.149
$x_1 \cdot x_2 \cdot x_3 \cdot x_4 \cdot x_5$	1	118	117.9	2.13	0.149
Error	64	3541	55.3		
Total	95	156,823			

Moreover, a multiple linear regression (MLR) is modeled to examine the main effects of factors on EC in Table 6. Also, the residuals of MLR are normally distributed. Moreover, $R^2 = 97.74\%$ and $R^2 = 93.89\%$ are obtained from ANOVA and MLR, respectively, verifying that both models properly fit the simulation results.

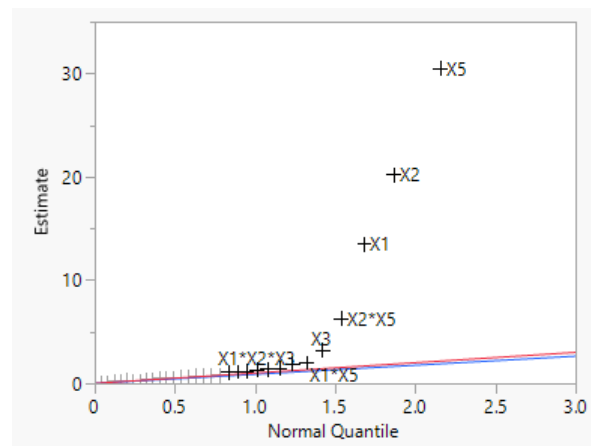


Figure 9. Half-normal plot of effects on the average EC.

Table 6. Multiple linear regression (MLR) results for the average EC.

$EC = b_0 + b_1 \cdot x_1 + b_2 \cdot x_2 + b_3 \cdot x_3 + b_4 \cdot x_4 + b_5 \cdot x_5 + b_{15} \cdot x_1 \cdot x_5 + b_{25} \cdot x_2 \cdot x_5 + b_{125} \cdot x_1 \cdot x_2 \cdot x_5$				
	Estimate	Std Error	t Ratio	Prob > t
Intercept	250.5	0.759149	330.02	<0.0001
x_1	13.5	0.759149	17.78	<0.0001
x_2	20.2	0.759149	26.63	<0.0001
x_3	3.2	0.759149	4.25	<0.0001
x_4	0.3	0.759149	0.41	0.6826
x_5	30.5	0.759149	40.22	<0.0001
$x_1 \cdot x_5$	-2.1	0.759149	-2.71	0.0087
$x_2 \cdot x_5$	-6.3	0.759149	-8.34	<0.0001
$x_1 \cdot x_2 \cdot x_5$	-1.9	0.759149	-2.53	0.0138

The ANOVA and MLR results also show that the number of forklifts (x_1), the number of S/R machines (x_2), the I/O buffer capacity of AS/RS (number of pallets) (x_3), and the flow rate (x_5) are statistically significant in deciding EC (p -value < 0.05), as in Tables 5 and 6. In particular, a switch from the DOE low level to the high level of x_5 significantly raises the with EC since it increases the proportion of pallets moving through Flows 2 and 3, with a great deal of traffic from a warehouse reserve area (AS/RS) to the warehouse forward area shown in Figure 7. Therefore, we observed more EC with the high-level x_5 since AS/RS is used more in comparison with the low-level x_5 . In this simulation, two types of transactions are defined to be processed by forklifts and S/R machines: storage and retrieval transactions. The retrieval transactions of AS/RS are controlled by x_3 among other factors. Larger x_3 requests more retrieval transactions from S/R machines, which significantly increases EC as shown in Tables 4 and 5; more S/R machines (x_2) or forklifts (x_1) can process more storage or retrieval transactions, which also significantly requires more EC at any given time moment. Table 5 suggests that order size (x_4) is the only insignificant factor for EC. This can be explained by the traffic-limiting effect of other factors. First, AS/RS activities are constrained by AS/RS I/O points (x_3), in which forklifts handle pallets toward the forward area or outbound docks. In other words, more utilization of AS/RS or S/R machines by more orders does not directly contribute to order deliveries at outbound docks. Therefore, order size x_4 is not likely to change AS/RS EC at a time due to this traffic-limiting effect of x_3 . Second, orders need to be delivered at outbound docks by forklifts from the cross-docking, reserve area, or forward area. Thus, the number of forklifts available (x_1) plays another traffic-limiting role in deciding EC even if x_4 increases. Overall, x_4 turns out to affect EC insignificantly or indirectly.

To minimize EC, it is also important that the main effects of the factors are analyzed with the interaction effects of factors. From the DOE results, x_5 also makes significant two-way and three-way interactions with x_1 and x_2 as in Table 6. For example, from all

Table 4 scenarios with x_2 and x_5 , the high-level x_5 (more use of AS/RS) with the high-level x_2 (more S/R machines) would result in the highest increase in EC, as suggested by Table 6: $30.5 (x_5 = 1) + 20.2 (x_2 = 1) - 2.1 (x_5 \cdot x_2 = 1) = 48.6$. Conversely, the minimum EC would be obtained if we select the low level of the experiment for both x_2 and x_5 . While an increase in both x_2 and x_5 raises the EC, individually, the combined (two-way interaction) effect of x_2 and x_5 is negative in this case. Figure 10 also provides the two-way interaction plot.

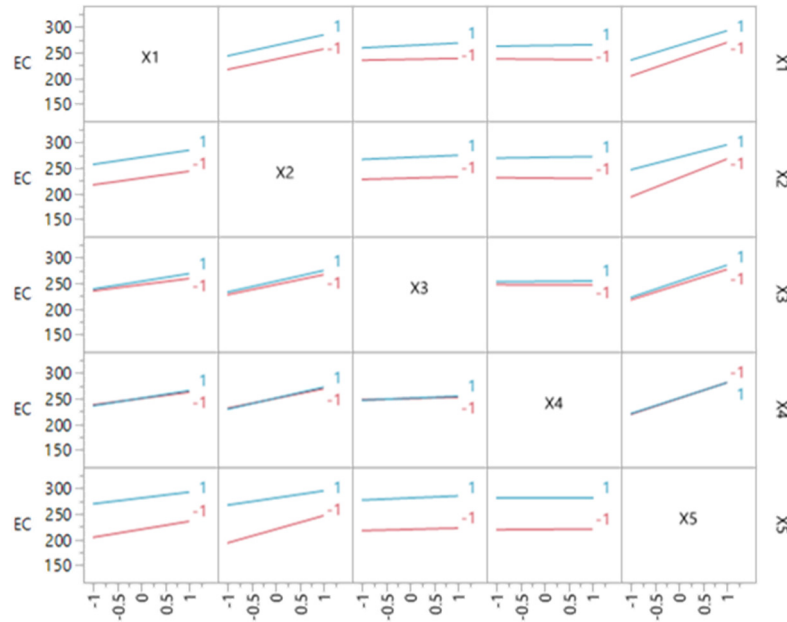


Figure 10. Two-way interaction plot for the average EC.

4.2. DOE for the OT of Integrated Energy-Aware Picker-to-Parts and Parts-to-Picker Systems

The results of 25 scenarios of the factorial design of the average OT are listed in Table 7. Also, the ANOVA and MLR results are presented in Tables 8 and 9, respectively. We modeled the MLR to analyze the main effects of the factors on the average OT. The normality assumption of model residuals is also met. Moreover, the ANOVA and MLR models fit the simulation results very well with $R^2 = 91.78\%$ and $R^2 = 83.60\%$, respectively. Figure 11 shows the half-normal plot of effects on average OT.

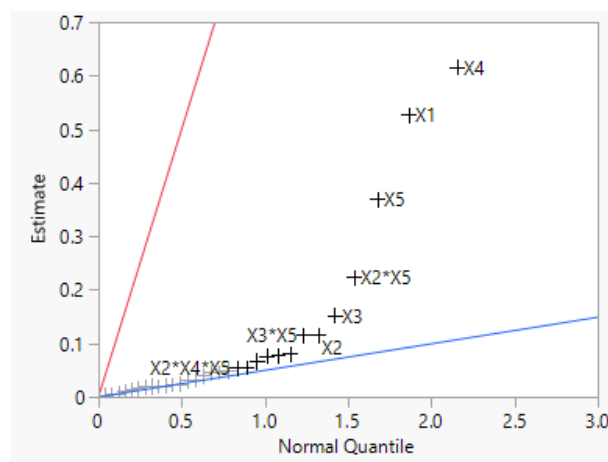


Figure 11. Half-normal plot of effects on the average OT.

Table 7. DOE results for the average OT of the integrated picker-to-parts and parts-to-picker systems.

Scenarios	Factors and Levels					Average OT (Hours)
	x_1	x_2	x_3	x_4	x_5	
1	-1	-1	-1	1	1	3.87
2	-1	-1	-1	-1	-1	2.29
3	-1	-1	1	1	1	3.56
4	-1	1	1	1	1	4.20
5	-1	1	-1	1	1	4.64
6	-1	-1	1	-1	1	2.68
7	-1	1	-1	-1	1	3.36
8	-1	-1	-1	-1	1	3.04
9	-1	-1	1	1	-1	3.53
10	-1	-1	-1	1	-1	3.19
11	-1	1	1	-1	1	2.72
12	-1	-1	1	-1	-1	2.38
13	-1	1	1	1	-1	3.39
14	-1	1	1	-1	-1	1.81
15	-1	1	-1	-1	-1	2.03
16	-1	1	-1	1	-1	3.00
17	1	1	-1	-1	1	2.52
18	1	1	-1	1	-1	2.67
19	1	1	1	-1	-1	0.65
20	1	-1	-1	-1	1	1.72
21	1	-1	1	1	1	2.09
22	1	1	1	-1	1	1.77
23	1	-1	1	-1	1	1.29
24	1	-1	-1	-1	-1	1.00
25	1	1	-1	1	1	3.95
26	1	-1	-1	1	1	2.63
27	1	-1	1	-1	-1	1.00
28	1	-1	1	1	-1	2.49
29	1	-1	-1	1	-1	2.65
30	1	1	1	1	1	3.14
31	1	1	1	1	-1	2.12
32	1	1	-1	-1	-1	1.14

From the ANOVA and MLR results, all main effects were found to be statistically significant. In terms of the order of absolute effect values, order size (x_4) significantly increases overdue orders and OT; larger x_4 requires more pallets to be delivered per order per given time as shown in Tables 8 and 9. In addition to x_4 , more forklifts (x_1) significantly decreased the OT by picking more orders in a shorter amount of time. Flow rate (x_5) is also a significant factor in a positive relationship with OT. If the low level of flow rate (x_5) switches to its high level in DOE, the proportion of pallets in a reserve area (AS/RS) increases when compared with the proportions in other warehouse areas as presented in Figure 7. This change results in more significant delays in delivering orders due to the longer storage time in the AS/RS as in Tables 8 and 9. Also, larger I/O AS/RS buffers (x_3) enable more pallets to move from the AS/RS to shipment, and this helps deliver more orders in a shorter time window and significantly reduces the OT according to the ANOVA and MLR results in Tables 8 and 9.

Table 8. ANOVA for the average OT of the integrated picker-to-parts and parts-to-picker systems.

Source	DF	Adj SS	Adj MS	F-Value	p-Value
Model	31	90.03	2.9042	17.08	0
Linear	5	79.832	15.9664	93.91	0
x_1	1	26.695	26.6947	157.01	0
x_2	1	1.288	1.2882	7.58	0.008
x_3	1	2.228	2.2276	13.1	0.001
x_4	1	36.499	36.4993	214.68	0
x_5	1	13.122	13.1223	77.18	0
Two-way interactions	10	8.965	0.8965	5.27	0
$x_1 \cdot x_2$	1	0.564	0.5638	3.32	0.073
$x_1 \cdot x_3$	1	0.624	0.6237	3.67	0.06
$x_1 \cdot x_4$	1	0.237	0.2367	1.39	0.242
$x_1 \cdot x_5$	1	0.105	0.1051	0.62	0.435
$x_2 \cdot x_3$	1	0.426	0.4263	2.51	0.118
$x_2 \cdot x_4$	1	0.579	0.5785	3.4	0.07
$x_2 \cdot x_5$	1	4.804	4.8036	28.25	0
$x_3 \cdot x_4$	1	0.05	0.0501	0.29	0.589
$x_3 \cdot x_5$	1	1.284	1.284	7.55	0.008
$x_4 \cdot x_5$	1	0.293	0.2934	1.73	0.194
Three-way interactions	10	1.112	0.1112	0.65	0.762
$x_1 \cdot x_2 \cdot x_3$	1	0.057	0.0573	0.34	0.563
$x_1 \cdot x_2 \cdot x_4$	1	0.035	0.0347	0.2	0.653
$x_1 \cdot x_2 \cdot x_5$	1	0.149	0.1493	0.88	0.352
$x_1 \cdot x_3 \cdot x_4$	1	0.212	0.2119	1.25	0.268
$x_1 \cdot x_3 \cdot x_5$	1	0.098	0.098	0.58	0.451
$x_1 \cdot x_4 \cdot x_5$	1	0.203	0.2028	1.19	0.279
$x_2 \cdot x_3 \cdot x_4$	1	0.039	0.0395	0.23	0.632
$x_2 \cdot x_3 \cdot x_5$	1	0.001	0.0013	0.01	0.931
$x_2 \cdot x_4 \cdot x_5$	1	0.29	0.2899	1.7	0.196
$x_3 \cdot x_4 \cdot x_5$	1	0.028	0.0278	0.16	0.687
Four-way interactions	5	0.118	0.0236	0.14	0.983
$x_1 \cdot x_2 \cdot x_3 \cdot x_4$	1	0.012	0.0118	0.07	0.793
$x_1 \cdot x_2 \cdot x_3 \cdot x_5$	1	0.018	0.0181	0.11	0.745
$x_1 \cdot x_2 \cdot x_4 \cdot x_5$	1	0.042	0.0424	0.25	0.619
$x_1 \cdot x_3 \cdot x_4 \cdot x_5$	1	0.041	0.0411	0.24	0.624
$x_2 \cdot x_3 \cdot x_4 \cdot x_5$	1	0.005	0.0045	0.03	0.871
Five-way interactions	1	0.002	0.002	0.01	0.913
$x_1 \cdot x_2 \cdot x_3 \cdot x_4 \cdot x_5$	1	0.002	0.002	0.01	0.913
Error	64	10.881	0.17		
Total	95	100.911			

Table 9. Multiple linear regression (MLR) results for the average OT.

$OT = b_0 + b_1 \cdot x_1 + b_2 \cdot x_2 + b_3 \cdot x_3 + b_4 \cdot x_4 + b_5 \cdot x_5 + b_{15} \cdot x_1 \cdot x_5 + b_{25} \cdot x_2 \cdot x_5$				
	Estimate	Std Error	t Ratio	Prob > t
Intercept	2.5772861	0.042083	61.24	<0.0001
x_1	-0.527323	0.042083	-12.53	<0.0001
x_2	0.1158388	0.042083	2.75	0.0077
x_3	-0.152328	0.042083	-3.62	0.0006
x_4	0.6166044	0.042083	14.65	<0.0001
x_5	0.3697165	0.042083	8.79	<0.0001
$x_1 \cdot x_5$	0.2236912	0.042083	5.32	<0.0001
$x_2 \cdot x_5$	-0.115649	0.042083	-2.75	0.0078

We observed that the number of S/R machines (x_2) is also a significant factor for OT from the results above. The effect of x_2 is positive as 0.1 is approximate, and this can be explained as x_2 is actually the number of S/R machines as well as the number of aisles

of the AS/RS to be used. In other words, we control the number of AS/RS aisles to be used by changing x_2 : when $x_2 = 1$, the number of S/R machines (the same as the number of AS/RS aisles to be used) is nine whereas the number is four with $x_2 = -1$. Thus, we can understand why a switch from -1 to $+1$ in x_2 does not improve the OT and actually increases the OT slightly since S/R machines or the number of AS/RS aisles available is not a traffic-limiting factor but rather a more resource-utilizing factor. In fact, the constraint of the I/O buffer capacity of the AS/RS (x_3) does not allow x_2 to contribute to OT. In other words, the I/O points of the AS/RS located between the reserve area and the forward area play bottleneck roles for the flow from the AS/RS to the forward area and shipment as in Figures 1 and 7. Therefore, more/fewer x_2 does not change the number of pallets from the reserve area (AS/RS) to be delivered for orders directly since the traffic is mostly controlled by x_3 . Also, x_5 is an important factor in determining OT, and the interaction term between x_2 and x_5 has a larger effect on the average OT than that of x_2 . Table 10 shows this point very clearly; the effect of x_2 is marginalized when x_5 and $x_2 \cdot x_5$ are considered together since the total effect from these three terms become negative only when x_5 is negative. Figure 12 visually presents other possible two-way interactions, including $x_2 \cdot x_5$.

Table 10. Effects of x_2 , x_5 , and $x_2 \cdot x_5$ on average OT.

Factor	x_2	x_5	$x_2 \cdot x_5$	Sum of Effects
Effects	0.115839	0.369717	0.223691	
Level	-1	1	-1	0.030187
	1	-1	-1	-0.47757
	-1	-1	1	-0.26186
	1	1	1	0.709247

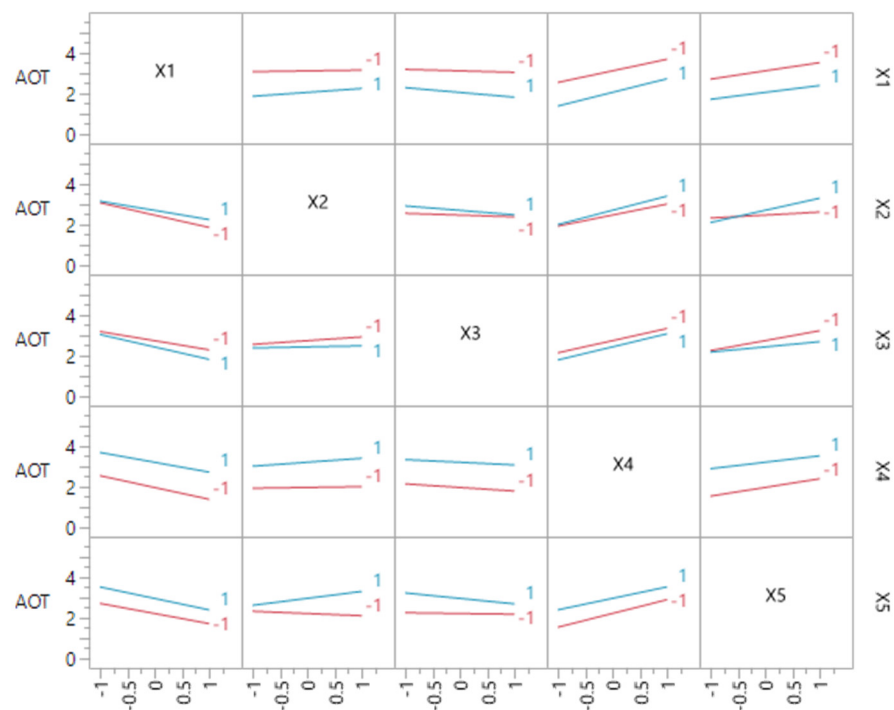


Figure 12. Two-way interaction plot for the average OT.

4.3. Pareto-Optimal DOE Scenarios

We used a Pareto-optimal front to analyze the results of 25 scenarios of two factorial designs conducted for EC and OT in one framework as in Figure 13. Thus, the Pareto-optimal front can be drawn with four non-dominated scenarios better than other scenarios

(dominated scenarios). No scenario represents a better quality than another in the Pareto-optimal front. From Table 11, we find that the low level is selected for the factor of flow rate (x_5) for all non-dominated scenarios. In other words, all non-dominated scenarios include a greater proportion of pallets through Flows 1 and 4 when compared with Flows 2 and 3, as shown in Figures 1 and 7. While the low DOE level of x_5 is designed to use AS/RS less with lower EC and OT, the high level of x_5 increases the use of AS/RS, resulting in more EC and OT by more AS/RS EC and storage time.

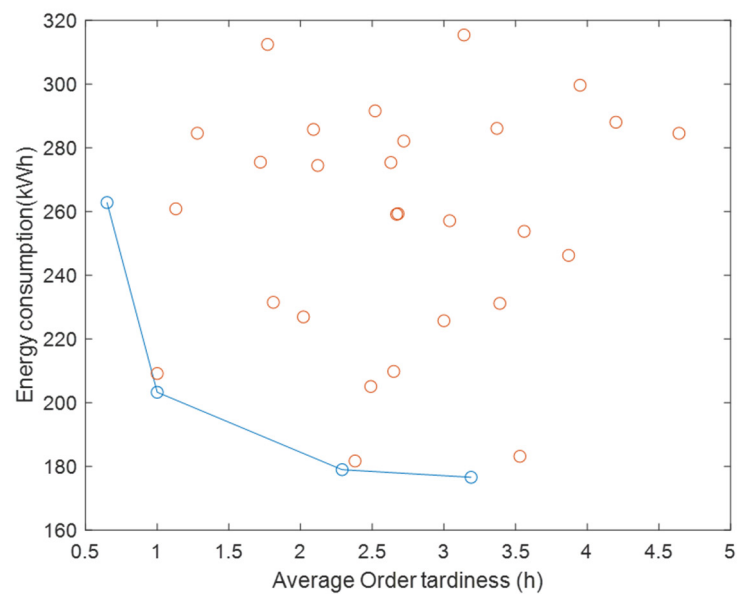


Figure 13. Pareto-optimal front plot for the 25 simulated scenarios.

Table 11. Non-dominated DOE scenarios for the integrated picker-to-parts and parts-to-picker system.

Scenarios	Factors and Levels					Mean of Responses	
	x_1	x_2	x_3	x_4	x_5	EC (kWh)	OT (Hours)
2	−1	−1	−1	−1	−1	178.96	2.29
10	−1	−1	−1	1	−1	176.56	3.19
19	1	1	1	−1	−1	262.79	0.65
24	1	−1	−1	−1	−1	203.25	1.00

5. Conclusions

In modern warehousing systems, it is crucial to investigate the trade-off between EC and OT while both reserve and forward areas are considered. For this, we analyzed five different important factors (the number of forklifts, the number of S/R machines, the I/O buffer capacity of the AS/RS, the order size, and the flow rate) affecting EC and OT to consider the interdependency between warehouse reserve and forward areas. We used simulation models to see how responses (EC and OT) act for different configurations of the five factors. Then, a 2^5 -factorial design was conducted for each EC and OT as DOE responses using the simulation. The results show that all factors significantly affect EC except the order size. Moreover, all factors were statistically significant in determining OT. Finally, we drew a Pareto-optimal front from the DOE results of EC and OT to provide multiple optimal scenarios for warehouse decision-makers. The four Pareto-optimal scenarios suggest that less traffic flows through a reserve area is the most important factor for Pareto-optimality.

These simulated results can be used by warehouse decision-makers to assess both sustainability and performance for each warehouse setting or configuration. In particular, this study presents that less traffic passing through a reserve area (Flows 1 and 4) can help

improve EC and OT at the same time while either level (+1 or −1) of the other factors (the number of forklifts, S/R machines, and AS/RS I/O points as well as order size) can impact EC and OT positively or negatively. Thus, this research suggests that the amount of traffic passing through a reserve area plays a significant role in improving both EC and OT.

While this study investigates the effects of warehouse factors on EC and OT, it has some possible improvements. This study utilizes all factors as binary variables, but further studies considering various factors as continuous variables deserve future research efforts. Also, other factors affecting the performance of warehouses can be additionally considered. For example, the dimensions of reserve and forward areas, including AS/RS size, can be varied. x_5 can be specified further in a future study. Currently, x_5 describes the flow difference between two cases with Flows 1 and 4 (high/low) and Flows 2 and 3 (low/high). Other possible combinations can be made and considered for x_5 .

Author Contributions: Conceptualization, H.-w.J. and A.E.; methodology, H.-w.J. and A.E.; software, H.-w.J. and A.E.; validation, H.-w.J. and A.E.; formal analysis, H.-w.J. and A.E.; investigation, H.-w.J. and A.E.; resources, H.-w.J. and G.-h.L.; data curation, H.-w.J.; writing—original draft preparation, H.-w.J. and A.E.; writing—review and editing, H.-w.J. and G.-h.L.; visualization, H.-w.J. and G.-h.L.; supervision, H.-w.J.; project administration, H.-w.J.; funding acquisition, H.-w.J. All authors have read and agreed to the published version of the manuscript.

Funding: This work was supported by the Korea Institute of Energy Technology Evaluation and Planning (KETEP) and the Ministry of Trade, Industry & Energy (MOTIE) of the Republic of Korea (2022400000260). This work was also supported by Institute of Information & communications Technology Planning & Evaluation (IITP) grant funded by the Korea government (MSIT) (No.RS-2022-00155911, Artificial Intelligence Convergence Innovation Human Resources Development (Kyung Hee University)).

Institutional Review Board Statement: Not applicable.

Informed Consent Statement: Not applicable.

Data Availability Statement: Not applicable.

Conflicts of Interest: The authors declare no conflict of interest. The funders had no role in the design of the study; in the collection, analyses, or interpretation of data; in the writing of the manuscript; or in the decision to publish the results.

Abbreviations

A/D	Acceleration/deceleration
ANOVA	Analysis of variance
AS/RS	Automated storage/retrieval system
AVS/RS	Vehicle storage and retrieval system
DOE	Design of experiments
EC	Energy consumption
I/O point	Input/output point
MLR	Multiple linear regression
OT	Order tardiness (average)
S/R	Storage and retrieval
SBS/RS	Shuttle-based storage and retrieval systems
SKU	Stock-keeping units

References

1. Young, L. Online Shopping's Fast-Delivery Race Is Slowing Down. *Wall Str. J.* 2023. Available online: <https://www.wsj.com/articles/online-shoppings-fast-delivery-race-is-slowing-down-73d4c68c> (accessed on 11 September 2023).
2. Ebrahimi, A.; Jeon, H.; Jung, S. Improving Energy Consumption and Order Tardiness in Picker-to-Part Warehouses with Electric Forklifts: A Comparison of Four Evolutionary Algorithms. *Sustainability* **2023**, *15*, 10551. [CrossRef]
3. Perotti, S.; Colicchia, C. Greening Warehouses through Energy Efficiency and Environmental Impact Reduction: A Conceptual Framework Based on a Systematic Literature Review. *Int. J. Logist. Manag.* **2023**. [CrossRef]

4. Füchtenhans, M.; Glock, C.H.; Grosse, E.H.; Zaroni, S. Using Smart Lighting Systems to Reduce Energy Costs in Warehouses: A Simulation Study. *Int. J. Logist. Res. Appl.* **2023**, *26*, 77–95. [[CrossRef](#)]
5. Heragu, S.S.; Du, L.; Mantel, R.J.; Schuur, P.C. Mathematical Model for Warehouse Design and Product Allocation. *Int. J. Prod. Res.* **2005**, *43*, 327–338. [[CrossRef](#)]
6. de Koster, R.; Le-Duc, T.; Roodbergen, K.J. Design and Control of Warehouse Order Picking: A Literature Review. *Eur. J. Oper. Res.* **2007**, *182*, 481–501. [[CrossRef](#)]
7. Yetkin Ekren, B. A Multi-Objective Optimisation Study for the Design of an AVS/RS Warehouse. *Int. J. Prod. Res.* **2021**, *59*, 1107–1126. [[CrossRef](#)]
8. Ekren, B.Y. A Simulation-Based Experimental Design for SBS/RS Warehouse Design by Considering Energy Related Performance Metrics. *Simul. Model. Pract. Theory* **2020**, *98*, 101991. [[CrossRef](#)]
9. Carli, R.; Dotoli, M.; Digiesi, S.; Facchini, F.; Mossa, G. Sustainable Scheduling of Material Handling Activities in Labor-Intensive Warehouses: A Decision and Control Model. *Sustainability* **2020**, *12*, 3111. [[CrossRef](#)]
10. Bortolini, M.; Faccio, M.; Ferrari, E.; Gamberi, M.; Pilati, F. Time and Energy Optimal Unit-Load Assignment for Automatic S/R Warehouses. *Int. J. Prod. Econ.* **2017**, *190*, 133–145. [[CrossRef](#)]
11. Meneghetti, A.; Monti, L. Sustainable Storage Assignment and Dwell-Point Policies for Automated Storage and Retrieval Systems. *Prod. Plan. Control* **2013**, *24*, 511–520. [[CrossRef](#)]
12. Lerher, T.; Edl, M.; Rosi, B. Energy Efficiency Model for the Mini-Load Automated Storage and Retrieval Systems. *Int. J. Adv. Manuf. Technol.* **2014**, *70*, 97–115. [[CrossRef](#)]
13. Stöhr, T.; Schadler, M.; Hafner, N. Benchmarking the Energy Efficiency of Diverse Automated Storage and Retrieval Systems. *FME Trans.* **2018**, *46*, 330–335. [[CrossRef](#)]
14. Tappia, E.; Marchet, G.; Melacini, M.; Perotti, S. Incorporating the Environmental Dimension in the Assessment of Automated Warehouses. *Prod. Plan. Control* **2015**, *26*, 824–838. [[CrossRef](#)]
15. Meneghetti, A.; Monti, L. Greening the Food Supply Chain: An Optimisation Model for Sustainable Design of Refrigerated Automated Warehouses. *Int. J. Prod. Res.* **2015**, *53*, 6567–6587. [[CrossRef](#)]
16. van den Berg, J.P.; Sharp, G.P.; Gademann, A.J.R.M.; Pochet, Y. Forward-Reserve Allocation in a Warehouse with Unit-Load Replenishments. *Eur. J. Oper. Res.* **1998**, *111*, 98–113. [[CrossRef](#)]
17. Lee, S.; Jeon, H.W.; Issabakhsh, M.; Ebrahimi, A. An Electric Forklift Routing Problem with Battery Charging and Energy Penalty Constraints. *J. Intell. Manuf.* **2021**, *33*, 1761–1777. [[CrossRef](#)]
18. Roodbergen, K.J.; Vis, I.F.A. A Survey of Literature on Automated Storage and Retrieval Systems. *Eur. J. Oper. Res.* **2009**, *194*, 343–362. [[CrossRef](#)]
19. Bartolini, M.; Bottani, E.; Grosse, E.H. Green Warehousing: Systematic Literature Review and Bibliometric Analysis. *J. Clean. Prod.* **2019**, *226*, 242–258. [[CrossRef](#)]
20. Facchini, F.; Mummolo, G.; Mossa, G.; Digiesi, S.; Boenzi, F.; Verriello, R. Minimizing the Carbon Footprint of Material Handling Equipment: Comparison of Electric and LPG Forklifts. *J. Ind. Eng. Manag. JIEM* **2016**, *9*, 1035–1046. [[CrossRef](#)]
21. Burinskiene, A.; Lorenc, A.; Lerher, T. A Simulation Study for the Sustainability and Reduction of Waste in Warehouse Logistics. *Int. J. Simul. Model.* **2018**, *17*, 485–497. [[CrossRef](#)]
22. Ekren, B.Y.; Heragu, S.S.; Krishnamurthy, A.; Malmberg, C.J. Simulation Based Experimental Design to Identify Factors Affecting Performance of AVS/RS. *Comput. Ind. Eng.* **2010**, *58*, 175–185. [[CrossRef](#)]
23. Marchet, G.; Melacini, M.; Perotti, S.; Tappia, E. Analytical Model to Estimate Performances of Autonomous Vehicle Storage and Retrieval Systems for Product Totes. *Int. J. Prod. Res.* **2012**, *50*, 7134–7148. [[CrossRef](#)]
24. Marchet, G.; Melacini, M.; Perotti, S.; Tappia, E. Development of a Framework for the Design of Autonomous Vehicle Storage and Retrieval Systems. *Int. J. Prod. Res.* **2013**, *51*, 4365–4387. [[CrossRef](#)]
25. Fichtinger, J.; Ries, J.M.; Grosse, E.H.; Baker, P. Assessing the Environmental Impact of Integrated Inventory and Warehouse Management. *Int. J. Prod. Econ.* **2015**, *170*, 717–729. [[CrossRef](#)]
26. Meneghetti, A.; Dal Borgo, E.; Monti, L. Rack Shape and Energy Efficient Operations in Automated Storage and Retrieval Systems. *Int. J. Prod. Res.* **2015**, *53*, 7090–7103. [[CrossRef](#)]
27. Manzini, R.; Accorsi, R.; Baruffaldi, G.; Cennerazzo, T.; Gamberi, M. Travel Time Models for Deep-Lane Unit-Load Autonomous Vehicle Storage and Retrieval System (AVS/RS). *Int. J. Prod. Res.* **2016**, *54*, 4286–4304. [[CrossRef](#)]
28. Lerher, T. Design of Experiments for Identifying the Throughput Performance of Shuttle-Based Storage and Retrieval Systems. *Procedia Eng.* **2017**, *187*, 324–334. [[CrossRef](#)]
29. Lerher, T.; Borovinsek, M.; Ficko, M.; Palcic, I. Parametric Study of Throughput Performance in SBS/RS Based on Simulation. *Int. J. Simul. Model.* **2017**, *16*, 96–107. [[CrossRef](#)]
30. Guerrazzi, E.; Mininno, V.; Aloini, D.; Dulmin, R.; Scarpelli, C.; Sabatini, M. Energy Evaluation of Deep-Lane Autonomous Vehicle Storage and Retrieval System. *Sustainability* **2019**, *11*, 3817. [[CrossRef](#)]
31. Ha, Y.; Chae, J. A Decision Model to Determine the Number of Shuttles in a Tier-to-Tier SBS/RS. *Int. J. Prod. Res.* **2019**, *57*, 963–984. [[CrossRef](#)]
32. Singhal, V.; Adil, G.K. A Simulation Analysis of Impact of Design and Storage Policy on Performance of Single-Crane Multi-Aisle AS/RS. *IFAC-Pap.* **2019**, *52*, 1620–1625. [[CrossRef](#)]

33. Xu, X.; Zhao, X.; Zou, B.; Gong, Y.; Wang, H. Travel Time Models for a Three-Dimensional Compact AS/RS Considering Different I/O Point Policies. *Int. J. Prod. Res.* **2019**, *58*, 5432–5455. [[CrossRef](#)]
34. Nia, A.R.; Far, M.H.; Niaki, S.T.A. A Hybrid Genetic and Imperialist Competitive Algorithm for Green Vendor Managed Inventory of Multi-Item Multi-Constraint EOQ Model under Shortage. *Appl. Soft Comput.* **2015**, *30*, 353–364.
35. Borovinšek, M.; Ekren, B.Y.; Burinskienė, A.; Lerher, T. Multi-Objective Optimisation Model of Shuttle-Based Storage and Retrieval System. *Transport* **2017**, *32*, 120–137. [[CrossRef](#)]
36. Yetkin Ekren, B.; Lerher, T. Energy and Cycle Time Efficient Warehouse Design for Autonomous Vehicle-Based Storage and Retrieval System. In Proceedings of the 14th IMHRC Proceedings, Karlsruhe, Germany, 12–16 June 2016.
37. Zajac, P. *Evaluation Method of Energy Consumption in Logistic Warehouse Systems*; Springer: Berlin/Heidelberg, Germany, 2015.
38. Hwang, H.; Lee, S.B. Travel-Time Models Considering the Operating Characteristics of the Storage and Retrieval Machine. *Int. J. Prod. Res.* **1990**, *28*, 1779–1789. [[CrossRef](#)]
39. TMHNA. Available online: <https://www.tmhna.com/> (accessed on 19 March 2023).
40. Jeon, H.W.; Taisch, M.; Prabhu, V. Measuring Variability on Electrical Power Demands in Manufacturing Operations. *J. Clean. Prod.* **2016**, *137*, 1628–1646. [[CrossRef](#)]
41. Scholz, A.; Schubert, D.; Wäscher, G. Order Picking with Multiple Pickers and Due Dates—Simultaneous Solution of Order Batching, Batch Assignment and Sequencing, and Picker Routing Problems. *Eur. J. Oper. Res.* **2017**, *263*, 461–478. [[CrossRef](#)]
42. Forklift Batteries: Conventional Vs. Fast Vs. Opportunity Charging. Available online: <https://www.tmhnc.com/blog/forklift-battery-charging-fast-opportunity-conventional> (accessed on 5 January 2023).

Disclaimer/Publisher’s Note: The statements, opinions and data contained in all publications are solely those of the individual author(s) and contributor(s) and not of MDPI and/or the editor(s). MDPI and/or the editor(s) disclaim responsibility for any injury to people or property resulting from any ideas, methods, instructions or products referred to in the content.